



## ORIGINAL ARTICLE

# CircBRD7 attenuates tumor growth and metastasis in nasopharyngeal carcinoma via epigenetic activation of its host gene

Jianxia Wei<sup>1,2,3</sup> | Mengna Li<sup>1,2,3</sup> | Shipeng Chen<sup>1,2,3</sup> | Changning Xue<sup>1,2,3</sup> |  
Lemei Zheng<sup>1,2,3</sup> | Yumei Duan<sup>1,2,3</sup> | Hongyu Deng<sup>1</sup> | Songqing Fan<sup>4</sup>  |  
Wei Xiong<sup>1,2,3</sup> | Ming Zhou<sup>1,2,3</sup> 

<sup>1</sup>NHC Key Laboratory of Carcinogenesis, Hunan Key Laboratory of Oncotarget Gene, Hunan Cancer Hospital and the Affiliated Cancer Hospital of Xiangya School of Medicine, Central South University, Changsha, China

<sup>2</sup>Cancer Research Institute and School of Basic Medical Sciences, Central South University, Changsha, China

<sup>3</sup>The Key Laboratory of Carcinogenesis and Cancer Invasion of the Chinese Ministry of Education, Central South University, Changsha, China

<sup>4</sup>Department of Pathology, the Second Xiangya Hospital, Central South University, Changsha, China

## Correspondence

Ming Zhou, Cancer Research Institute, Central South University, 110 Xiangya Road, Changsha, Hunan 410078, China.  
Email: [zhouming2001@163.com](mailto:zhouming2001@163.com)

## Funding information

National Natural Science Foundation of China, Grant/Award Number: 82172592; Project 211, Grant/Award Number: 111-2-12

## Abstract

BRD7 was identified as a tumor suppressor in nasopharyngeal carcinoma (NPC). Circular RNAs (CircRNAs) are involved in the occurrence and development of NPC as oncogenes or tumor suppressors. However, the function and mechanism of the circular RNA forms derived from BRD7 in NPC are not well understood. In this study, we first identified that circBRD7 was a novel circRNA derived from BRD7 that inhibited cell proliferation, migration, invasion of NPC cells, as well as the xenograft tumor growth and metastasis in vivo. Mechanistically, circBRD7 promoted the transcriptional activation and expression of BRD7 by enhancing the enrichment of histone 3 lysine 27 acetylation (H3K27ac) in the promoter region of its host gene BRD7, and BRD7 promoted the formation of circBRD7. Therefore, circBRD7 formed a positive feedback loop with BRD7 to inhibit NPC development and progression. Moreover, restoration of BRD7 expression rescued the inhibitory effect of circBRD7 on the malignant progression of NPC. In addition, circBRD7 demonstrated low expression in NPC tissues, which was positively correlated with BRD7 expression and negatively correlated with the clinical stage of NPC patients. Taken together, circBRD7 attenuates the tumor growth and metastasis of NPC by forming a positive feedback loop with its host gene BRD7, and targeting the circBRD7/BRD7 axis is a promising strategy for the clinical diagnosis and treatment of NPC.

## KEYWORDS

BRD7, circBRD7, host gene, nasopharyngeal carcinoma, tumor progression

## 1 | INTRODUCTION

Nasopharyngeal carcinoma (NPC) is a malignant head and neck tumor originating from the nasopharynx epithelium that has become a serious public health problem due to its high recurrence rate and

high metastasis rate.<sup>1-3</sup> Bromodomain-containing protein 7 (BRD7) is a novel gene cloned early by our group through complementary DNA (cDNA) representative difference analysis and was identified as a critical member of the bromodomain protein family.<sup>4,5</sup> Previous studies have found that BRD7 is significantly downregulated in NPC

This is an open access article under the terms of the [Creative Commons Attribution-NonCommercial](https://creativecommons.org/licenses/by-nc/4.0/) License, which permits use, distribution and reproduction in any medium, provided the original work is properly cited and is not used for commercial purposes.

© 2023 The Authors. *Cancer Science* published by John Wiley & Sons Australia, Ltd on behalf of Japanese Cancer Association.

tissues and has the function of inhibiting cell proliferation, tumor growth and metastasis of NPC by negatively regulating the Rb/E2F, PI3K/AKT, and Wnt/ $\beta$ -catenin pathways, thus exerting tumor suppressive role in NPC.<sup>6-10</sup>

Circular RNAs (CircRNAs) are a novel class of non-coding RNAs that form a covalently closed loop through exon skipping or back-splicing.<sup>11,12</sup> CircRNAs are considered to be stable, conserved, and abundant compared to traditional linear RNAs. Increasing evidence shows that circRNAs participate in the occurrence and progression of NPC as oncogenes or tumor suppressors.<sup>13-17</sup> However, the function and mechanism of the circRNA derived from the BRD7 in NPC are not well understood. Therefore, exploring the circular form of BRD7 is helpful to further ascertain the mechanism by which the BRD7 gene is involved in NPC.

In the present study, circBRD7 was first identified as a novel circRNA derived from BRD7 that attenuates cell proliferation, tumor growth, and metastasis by promoting the transcriptional activation and expression of its host gene. In addition, circBRD7 was expressed at low levels in NPC tissues and correlated with BRD7 expression as well as the clinical stages of NPC patients. Therefore, targeting the circBRD7/BRD7 axis is a promising strategy for the clinical diagnosis and treatment of NPC.

## 2 | MATERIALS AND METHODS

### 2.1 | Clinical tissue samples

All noncancerous nasopharyngeal epithelial (NPE) tissues and NPC tissues were paraffin-embedded and collected from the Second Xiangya Hospital of Central South University (Changsha, China). All tissues for experimental use were collected with the authorization of the Ethics Committee of Central South University, and written informed consent was obtained from the patients.

### 2.2 | Cell lines and cell culture

Nasopharyngeal carcinoma cell lines 5-8F and 6-10B were kindly provided by the Cancer Center of Sun Yet-Sen University

(Guangzhou, China) and preserved in our laboratory. The human normal NPE cell line NP69 and NPC cell lines CNE1, CNE2, HNE1, HNE2, HONE1, and HK1 were purchased from the Cell Center of Xiangya School of Medicine at Central South University (Changsha, China). All NPC cells mentioned above were cultured in DMEM (Life Technologies) supplemented with 10% FBS (BI, Jerusalem, Israel) at 37°C and contained 5% CO<sub>2</sub> atmosphere. NP69 was cultured in Defined Keratinocyte-SFM (1×, Gibco, USA). CELLSAVING (New Cellular and Molecular Biotech) was used for cell freezing storage.

### 2.3 | Cell transfection

A plasmid overexpressing circBRD7 was constructed by fusing the whole-length circBRD7 sequence into pcDNA3.1(+) circRNA Mini plasmid. CircBRD7 siRNAs (sicircBRD7#1 and sicircBRD7#2), BRD7 siRNAs (siBRD7#1 and siBRD7#2), and miRNA mimics (hsa-miR-498 and hsa-miR-944) were purchased from RiboBio (Guangdong, China). The sequences of the circBRD7 siRNAs were as follows: sicircBRD7#1: 5'-AGUUAUCCUGACUGUUCACdTdT-3'; sicircBRD7#2: 5'-UUUGAAGUUAUCCUGACUGdTdT-3'. The sequences of siBRD7#1 and siBRD7#2 were described in our previous publication.<sup>18</sup> In this paper, we used the pool of these two BRD7 siRNAs to perform recovery experiments. The 5-8F and CNE2 cells were seeded in six-well plates, and then the plasmids, siRNAs, and microRNA mimics were transfected into these above cells using Lipofectamine 3000 Reagent (Invitrogen, USA) according to the manufacturer's instructions, respectively.

### 2.4 | RT-PCR and quantitative real-time PCR

Total RNA was extracted from cell lines and tissues using AG RNAex Pro Reagent (Accurate Biology) and subjected to reverse transcription by applying the reverse transcription kit (Thermo Scientific). Real-time PCR was performed with the ChamQ Universal SYBR qPCR Master Mix qPCR Kit (Vazyme), and GAPDH or U6 was used as an endogenous control. The RT-qPCR primer sequences used for the detection of BRD7, circBRD7, and other potential circRNAs derived from BRD7 are listed in Table 1 and

Name	Sequences (5'-3')	Primer Length (bp)
BRD7-Forward	ATGAGACCACCAGATTGC	18
BRD7-Reverse	TCCATACGTGCTTACGAT	18
circBRD7-Forward	CGTGAAGGAATCTGGAGGAA	20
circBRD7-Reverse	TCATTCTGAGTGCAACAGC	20
GAPDH-Forward	CAACGGATTGGTCGTATTGG	21
GAPDH-Reverse	TGACGGTGCCATGGAATTT	19
U6-Forward	ATTGGAACGATACAGAGAAGATT	23
U6-Reverse	GGAACGCTTACGAATTTG	19

TABLE 1 The RT-qPCR primer sequences used for the detection of BRD7 and circBRD7.

**Table S1**, respectively. For miRNA detection, a miDETECT A Track™ miRNA qRT-PCR Starter kit (RiboBio, Guangzhou, China) was used for reverse transcription and RT-qPCR, and U6 was used as the internal reference. The RT-qPCR primer sequences used for the detection of miR-498 and miR-944 are listed in **Table S2**. The relative expression of target genes was calculated with the  $2^{-\Delta\Delta CT}$  method.

## 2.5 | FISH

The FISH digoxigenin-labeled specific probe targeting circBRD7 was designed and synthesized by Sangon Biotech (Shanghai, China), and the sequence was 5'-TAGTTTGAAGTTATCCTGACTGTTTCAAG-3'. The FISH assay was performed according to the manufacturer's instructions (GenePharma, China). First, cells were fixed in 4% paraformaldehyde and permeabilized with 0.25% Triton X-100 at room temperature for 15 min. Thereafter, cells were hybridized with the FISH probe in hybridization buffer at 37°C overnight. Finally, the cells were stained with DAPI and photographed using a confocal microscope (Perkin-Elmer).

## 2.6 | Cell counting kit-8 and colony formation assays

For the cell counting kit-8 (CCK-8) assay,  $1 \times 10^3$  cells/well were seeded into 96-well plates. CCK-8 reagent (Selleck) was added to each well and incubated for 2 h at the indicated time points (0, 1, 2, 3, 4, and 5 days). Then, the absorbance at 450 nm was measured with a microplate analyzer (Beckman). For the colony formation assay,  $1 \times 10^3$  cells/well were plated into six-well plates. The cells were allowed to grow for 1 to 2 weeks, and the colonies were observed with crystal violet staining.

## 2.7 | Cell cycle and cell apoptosis

The cell cycle analysis was described in our previous work. For cell cycle analysis, cells were harvested and fixed in 70% ethanol for 24 h at  $-20^\circ\text{C}$ . The cells were then treated with RNase A and stained with 25  $\mu\text{g/mL}$  propidium iodide (PI).<sup>18</sup> For cell apoptosis analysis, 24 h after cell transfection, cells were treated with serum starvation for 24 h, and then the ratio of apoptotic cells was determined using an Annexin V-FITC/PI double staining kit (4A Biotech, Beijing, China).

## 2.8 | Wound healing and transwell assays

Cells were seeded in six-well plates, and then a 10  $\mu\text{L}$  plastic pipette tip was used to create a straight scratch through the cell monolayer when the cells grew to approximately 90% confluence. Images of

the scratch width were acquired at 0, 12, and 24 h after the initial scratch, and the area of cell migration was measured by using Image J software. For transwell assays, Matrigel (BD, Franklin Lakes, NJ, USA) was diluted using serum-free medium at a ratio of 8:1 and then added to the transwell chamber (Millipore) for 3 h. Then 600  $\mu\text{L}$  of medium containing 20% FBS was added to the lower chamber. After that,  $5 \times 10^4$  cells were suspended in 200  $\mu\text{L}$  of serum-free medium and added to the top chamber. After incubation at  $37^\circ\text{C}$  for 48 h, the cells were fixed with 4% paraformaldehyde and stained with crystal violet, and the number of migrated cells was counted using Image J software.

## 2.9 | Luciferase reporter assay

The pGL3 enhancer and pRL-TK vectors were purchased from Promega (Fitchburg, WI, USA). The recombinant reporter vector fused with the BRD7 promoter (pGL3 enhancer/BRD7 promoter) was constructed for the evaluation of BRD7 promoter activity. Cells were co-transfected with the pcDNA3.1(+) circRNA vector or circ-BRD7 overexpression plasmid, and the pRL-TK was used as an internal control. Cells were harvested following transfection for 48 h and analyzed by utilizing the Dual-Luciferase Reporter Assay system (Promega) according to the manufacturer's instructions. Firefly luciferase activity was normalized to Renilla luciferase activity.

## 2.10 | ChIP

ChIP was performed according to the introduction of our previous.<sup>19</sup> Briefly, cells were crosslinked with 1% formaldehyde and then harvested and lysed. Nuclei lysis buffer was added to the precipitate and the chromatin was broken up into fragments of 100–500 bp by a BioRuptor sonicator (Diagenode). Chromatin was immunoprecipitated with immunoglobulin IgG (Sigma) and anti-histone 3 lysine 27 acetylation (H3K27ac) antibody (ABclonal) with the Protein A/G Magnetic Beads system (Selleck Chemicals) according to the manufacturer's protocols. Finally, the collected DNA was used for subsequent RT-qPCR. The primer sequences used for the ChIP-qPCR assay are listed in **Table 2**.

## 2.11 | Western blot

The detailed method of western blot has been published.<sup>18,20</sup> Primary antibodies used in western blot are as follows: anti-BRD7 (Proteintech), anti-CDK4 (Proteintech), anti-GAPDH (Proteintech), anti-p21 (CST, MA, USA), anti-Snail (CST, MA, USA), anti-E-cadherin (CST, MA, USA), anti-N-cadherin (CST, MA, USA), and anti-Vimentin (Arigo). The protein bands were revealed by enhanced chemiluminescence reagent (Millipore) following the manufacturer's recommendations, and captured by chemiluminescence imaging systems (MiniChemiluminescence I, SAGECREATION, China).

Name	Sequences (5'-3')	Primer Length (bp)
ChIP-P1-Forward	GCTCCTACTGAAGCCCAAGTT	21
ChIP-P1-Reverse	CGAGATAAGGGGACACCCTTTAA	23
ChIP-P2-Forward	TTATCTCGTCCTGGGGGA	18
ChIP-P2-Reverse	TTACTCATCAGGGCGATGC	19
ChIP-P3-Forward	ATGAGTAAGCTGGACGGCAT	20
ChIP-P3-Reverse	AATTGTCCAACCTGCTGAGC	19
ChIP-P4-Forward	GCTCAGCAGTTGGACAATTATTC	23
ChIP-P4-Reverse	GTATTAACAAAGGCCTGGC	19

**TABLE 2** The primer sequences for ChIP-qPCR assay.

## 2.12 | In situ hybridization and immunohistochemistry staining

For in situ hybridization (ISH) staining, the ISH kit was purchased from Boster Biological (Wuhan, China) and used according to the manufacturer's instructions. Immunohistochemical staining (IHC) staining was performed as previously described by the research group.<sup>20</sup> Sections were incubated with anti-BRD7 (Proteintech), anti-p21 (CST, MA, USA), anti-CDK4 (Proteintech), anti-Ki67 (Bioworld), anti-Vimentin (Arigo), and anti-E-cadherin (Abclonal). MaxVision™ HRP-Polymer anti-Mouse/Rabbit was incubated at room temperature for 30 min. After DAB staining, the nuclei were counterstained with hematoxylin (Solarbio). The results of ISH and IHC were analyzed according to the staining intensity and distribution of stained cells.<sup>20,21</sup> The final score is the product of the intensity score and positive rate score. The expression level was classified as low or high with the median total score as the cutoff.

## 2.13 | In vivo nude mouse models

The five-week-old female BALB/C nude mice used were purchased from Hunan Slyke Jingda Experimental Animal Co., Ltd. All animals were fed in an Specific Pathogen Free (SPF) level barrier system of the Laboratory Animal Science Department of Central South University. For the xenograft tumor model, the nude mice were randomly divided into three groups ( $n=5$  per group): 5-8F/Ctrl, 5-8F/circBRD7, and 5-8F/circBRD7 plus siBRD7. A total of  $5 \times 10^6$  transfected 5-8F cells in 150  $\mu$ L of saline were inoculated into the right subcutaneous position of each nude mouse. Tumor size and volume were observed and measured every 3 days after injection. The tumor volume was calculated according to the following formula:  $\text{volume} = (\text{length} \times \text{width}^2) \times 1/2$ . After 30 days of subcutaneous inoculation, all nude mice were killed. The tumors were removed and weighed, fixed with 4% paraformaldehyde, and preserved after paraffin embedding. For the lung metastatic tumor model, the nude mice were divided into three groups ( $n=7$  per group): 5-8F/Ctrl, 5-8F/circBRD7, and 5-8F/circBRD7 plus siBRD7. A total of  $3 \times 10^6$  5-8F cells in 200  $\mu$ L of saline were injected into nude mice via the tail vein. Eight weeks later, the lung tissues were removed, and the

number of nodules was observed and recorded. Then, the lung tissues were fixed with 4% paraformaldehyde, dehydrated by gradient alcohol, embedded in paraffin, and sectioned for H&E staining.

## 2.14 | Statistical analysis

GraphPad Prism 7.0 software was applied for statistical analysis. All data in this study were expressed as mean  $\pm$  SEM. Student's *t*-test was used to analyze the significant differences between the two groups of data. One-way ANOVA was used to analyze differences among multiple sets of data. Correlations were evaluated by Pearson correlation analysis. *p* values  $<0.05$  were considered statistically significant (ns, no significance; \* $p < 0.05$ ; \*\* $p < 0.01$ ; \*\*\* $p < 0.001$ ).

## 3 | RESULTS

### 3.1 | CircBRD7 was identified as a circular RNA encoded by its host gene BRD7

To confirm whether BRD7 has a circular RNA form in NPC, we predicted the circRNAs encoded by the BRD7 gene through bioinformatics analysis and found that BRD7 may encode five potential circRNAs, as shown in Figure S1A. Among them, hsa\_circ\_0039345 was amplified to the reverse splicing site sequence by RT-qPCR (Figure S1B). Moreover, circ\_0039345 could be detected by the amplification of divergent primers in cDNA but not in genomic DNA from NPC cells, confirming that circ\_0039345 is a true circRNA from BRD7, and it was named circBRD7 (Figure 1A). Sanger sequencing confirmed that circBRD7 was formed by reverse splicing of exons 6–8 of the BRD7, with a full length of 420 bp (Figure 1B). Subsequently, RT-qPCR results revealed significantly lower expression of circBRD7 in NPC cell lines than in the normal NPE cell line NP69 (Figure 1C). RNA fluorescence in situ hybridization (FISH) and nucleoplasmic separation experiments showed that circBRD7 was distributed in both the nucleus and cytoplasm of NPC cell lines, with the majority in the nucleus (Figure 1D,E). To test the stability of circBRD7, we treated 5-8F and CNE2 cells with actinomycin D to inhibit intracellular RNA transcription and then extracted total RNA for



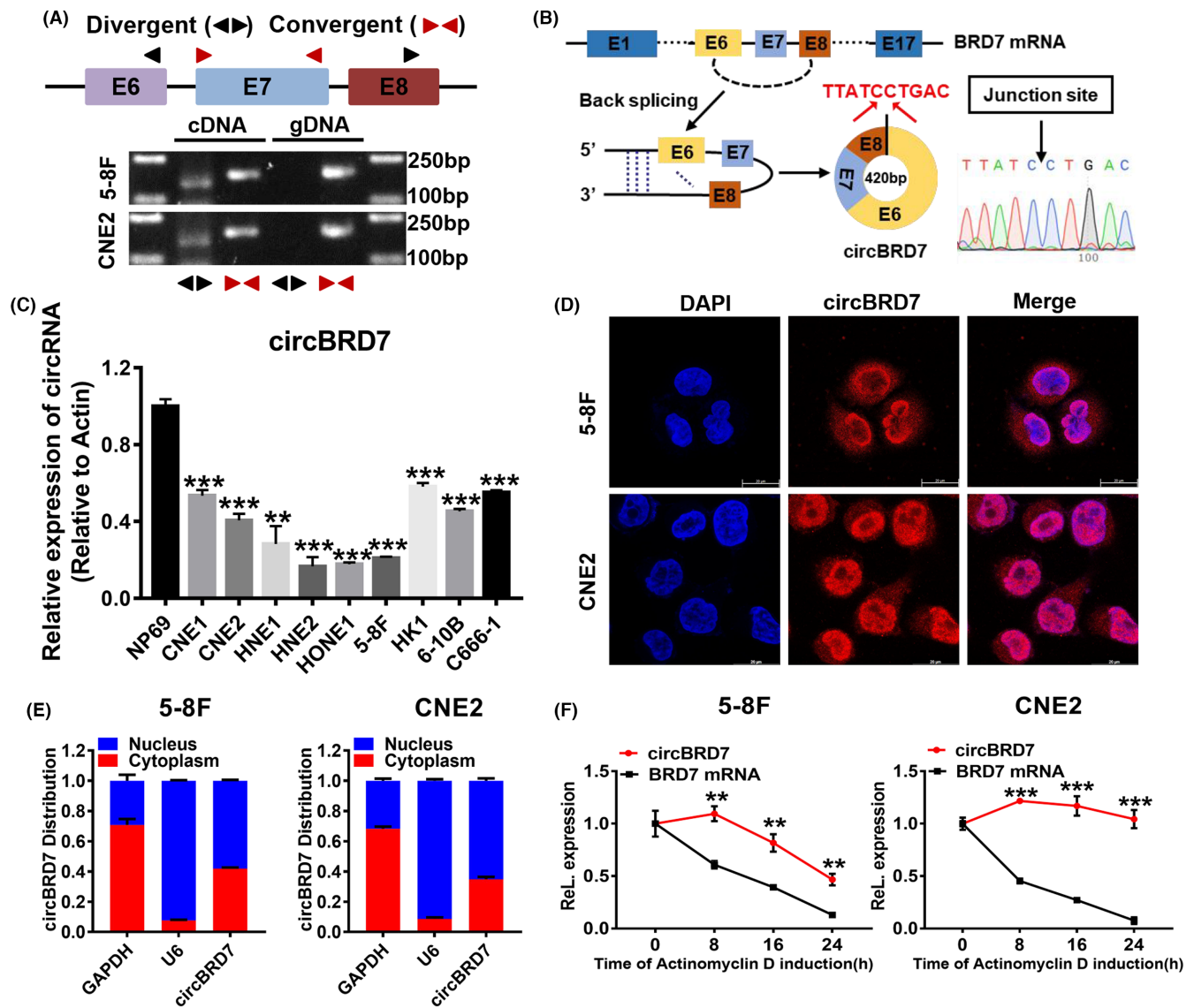


**FIGURE 1** CircBRD7 was identified as a circular RNA encoded by its host gene BRD7. (A) Agarose gel electrophoresis identified circ\_0039345 fragments amplified in complementary DNA (cDNA) and genomic DNA (gDNA) using divergent primer and convergent primer. (B) The back-splicing junction and total length of circBRD7 were validated by Sanger sequencing. (C) RT-qPCR was used to detect the expression of circBRD7 in nine nasopharyngeal carcinoma (NPC) cell lines and normal NPE cell NP69. Actin served as an internal control. (D) Intracellular localization of circBRD7 in 5-8F and CNE2 cells was detected by FISH. Nuclei were stained with DAPI. Scale bar, 20 μm. (E) The expression of circBRD7 in cytoplasm and nucleus was detected by nucleo-cytoplasmic separation assay. GAPDH, cytoplasmic marker; U6, nuclear marker. (F) The stability of circBRD7 and BRD7 was detected in actinomycin D-treated 5-8F and CNE2 cells using RT-qPCR. Data are presented as mean ± SEM. \*\* $p < 0.01$ ; \*\*\* $p < 0.001$ .

RT-qPCR detection. As a result, circBRD7 was more stable than the linear mRNA encoded by the BRD7 gene (Figure 1F). These results indicated that circBRD7 is a circular RNA derived from its host gene.

### 3.2 | CircBRD7 attenuates cell proliferation and cell cycle progression

To investigate the function of circBRD7 in NPC, we constructed NPC 5-8F and CNE2 cell models with circBRD7 overexpression

or knockdown, respectively, and RT-qPCR results showed that overexpression or knockdown of circBRD7 resulted in better overexpression or silencing efficiency in these cell models (Figure 2A and Figure S2A). CCK-8 and colony formation experiments showed that overexpression of circBRD7 inhibited the cell proliferation and colony formation of NPC cells. Conversely, silencing circBRD7 promoted the proliferation and colony formation of NPC cells (Figure 2B,C and Figure S2B,C). To clarify its potential cellular biological mechanism, a flow cytometry assay was performed to investigate the effect of circBRD7 on the NPC

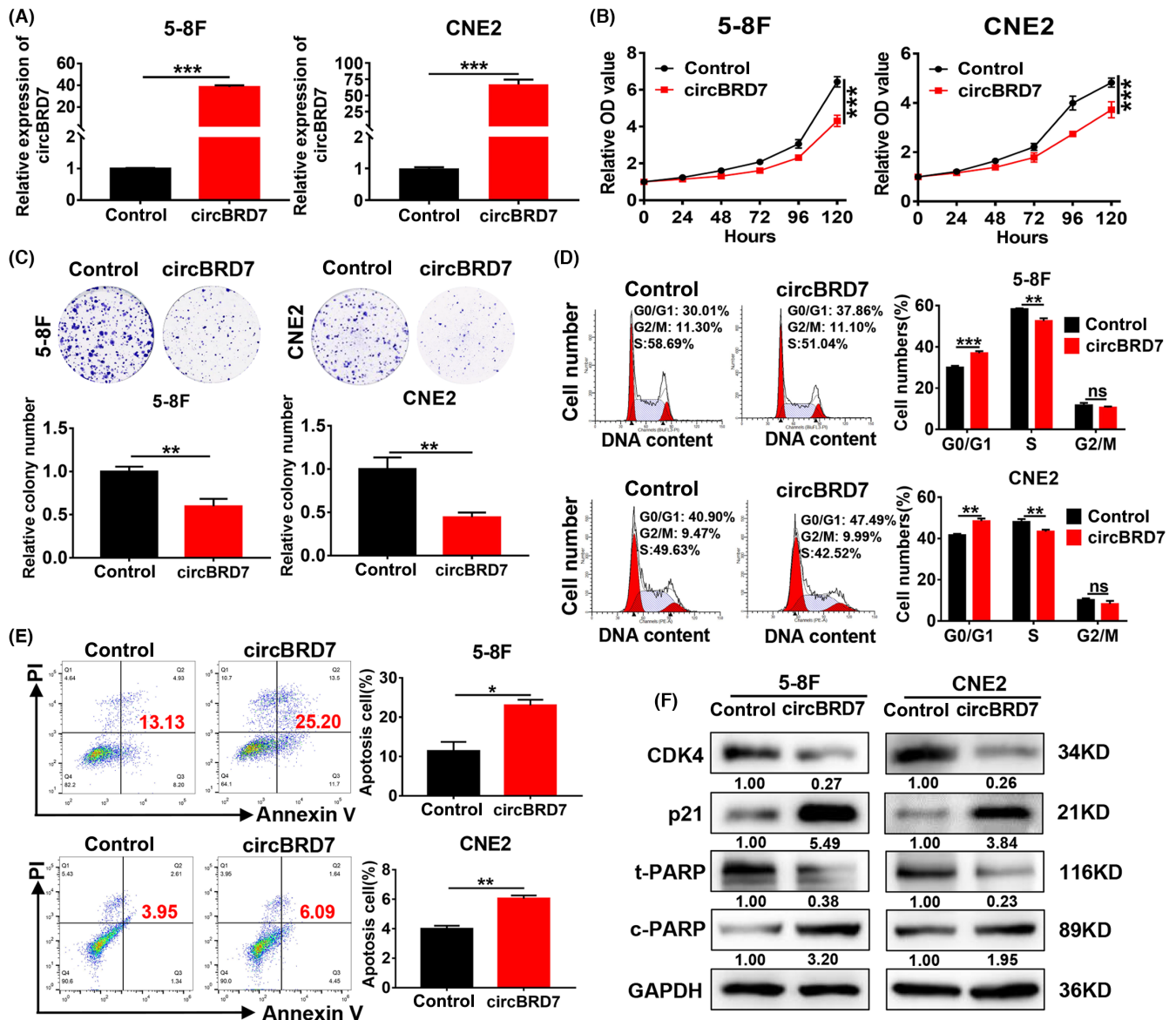


**FIGURE 2** CircBRD7 inhibits cell proliferation and cell cycle progression of nasopharyngeal carcinoma (NPC) cells. (A) RT-qPCR assay was used to detect the expression efficiency of circBRD7 overexpressed vector in 5-8F and CNE2 cells. (B, C) Cell counting kit-8 (CCK-8) (B) and colony formation (C) assays were used to detect the effect of circBRD7 overexpression on the proliferation and colony formation abilities of 5-8F and CNE2 cells. (D, E) Flow cytometry was performed to detect the effect of circBRD7 overexpression on the cell cycle process (D) and cell apoptosis (E) of NPC cells. (F) Western blot assay was used to detect the expression of cyclin-related molecules CDK4, p21, and apoptosis-related molecules t-PARP and c-PARP, with GAPDH as normalized control. Data are presented as mean  $\pm$  SEM. \* $p < 0.05$ ; \*\* $p < 0.01$ ; \*\*\* $p < 0.001$ ; ns, no significance.

cell cycle. As a result, overexpression of circBRD7 obviously inhibited cell cycle progression from G1 to S, arrested more cells at the G0/G1 phase (Figure 2D), and promoted cell apoptosis in NPC cells (Figure 2E). Furthermore, overexpression of circBRD7 promoted the expression of p21 but inhibited that of CDK4 and promoted the expression of the apoptosis marker c-PARP; however, silencing circBRD7 had the opposite effect (Figure 2F, Figures S3 and S2D). Taken together, these results indicated that circBRD7 attenuates cell proliferation and cell cycle G1/S progression and initiates cell apoptosis in NPC cells, thus playing a tumor suppressor role in NPC.

### 3.3 | CircBRD7 inhibits cell migration, invasion, and epithelial-mesenchymal transition of nasopharyngeal carcinoma cells

To fully clarify the biological functions of circBRD7 in NPC, we further detected the effect of circBRD7 on the migration, invasion, and epithelial-mesenchymal transition (EMT) of NPC cells. Wound healing test results demonstrated that overexpression of circBRD7 significantly weakened the migration ability of NPC cells (Figure 3A), whereas silencing circBRD7 promoted the migration of NPC cells (Figure S4A). The results of the transwell assay revealed

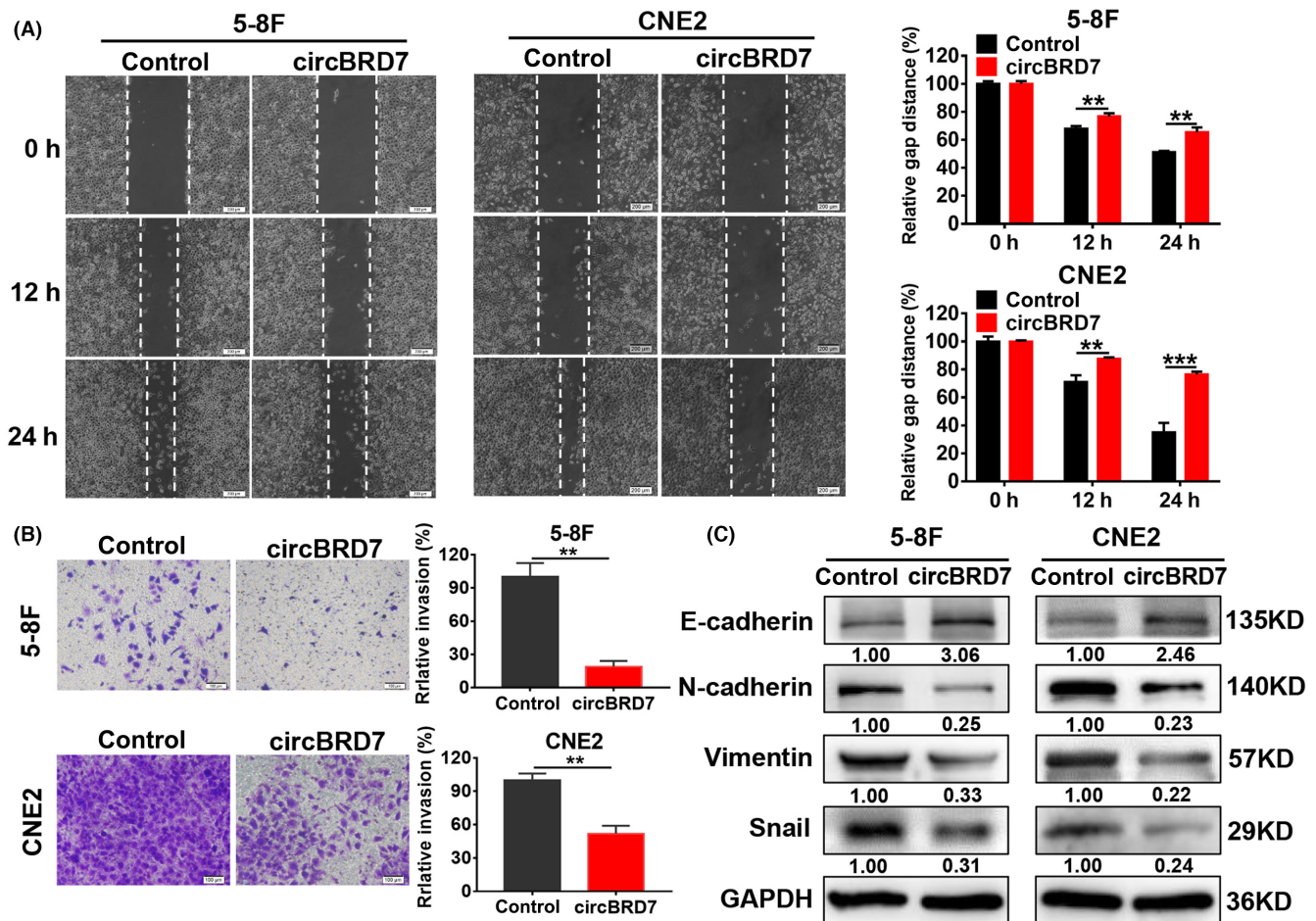


**FIGURE 3** CircBRD7 inhibits cell migration, invasion, and epithelial-mesenchymal transition (EMT) of nasopharyngeal carcinoma (NPC) cells. (A, B) Representative and quantified results of the wound healing (A) and transwell (B) assays in 5-8F and CNE2 cells transfected with circBRD7 overexpression plasmid or blank vector. (C) Western blot was used to analyze the expression of EMT-related molecules E-cadherin, N-cadherin, Vimentin, and Snail before and after circBRD7 overexpression. Data are presented as mean  $\pm$  SEM. \*\* $p < 0.01$ ; \*\*\* $p < 0.001$ ; ns, no significance.

that overexpression of circBRD7 significantly inhibited the invasion ability of 5-8F and CNE2 cells (Figure 3B), while silencing circBRD7 had the opposite effect (Figure S4B). Western blot data illustrated that the level of the epithelial marker E-cadherin was increased after circBRD7 overexpression, while the mesenchymal markers N-cadherin, Vimentin, and Snail were decreased (Figure 3C and Figure S5), whereas silencing circBRD7 presented the opposite result (Figure S4C), which demonstrated that circBRD7 inhibits migration and EMT in NPC cells.

### 3.4 | CircBRD7 promotes the transcriptional activation and expression of its host gene

Emerging studies have documented that the regulation of circRNA on its host gene is an important molecular mechanism for its function.<sup>22-25</sup> Herein, we first investigated the regulatory effect and mechanism of circBRD7 on the expression of its host gene. RT-qPCR and western blot assays indicated that overexpression of circBRD7

caused an increase in the mRNA and protein expression of BRD7, whereas silencing circBRD7 reduced BRD7 expression (Figure 4A,B). The biological function of circRNA is closely related to its subcellular localization, given that circBRD7 is mainly located in the cell nucleus (Figure 1D,E) and positively regulates the mRNA expression of its host gene, implying that circBRD7 may mainly regulate BRD7 expression through the transcriptional mechanism. Subsequently, we constructed a luciferase reporter vector containing the potential promoter sequence of BRD7 predicted by bioinformatic analysis, and the dual-luciferase reporter assay showed that the BRD7 potential promoter had significant promoter activity and overexpression of circBRD7 enhanced BRD7 promoter activity (Figure 4C,D), suggesting that circBRD7 upregulates the promoter activity of its host gene.

Histone 3 lysine 27 acetylation and histone H3 lysine 4 trimethylation (H3K4me3) are common post-translational modifications of histones that can transcriptionally activate gene expression in adjacent regions by affecting the chromatin opening state.<sup>26-28</sup> To this end, we analyzed the transcriptional modification region

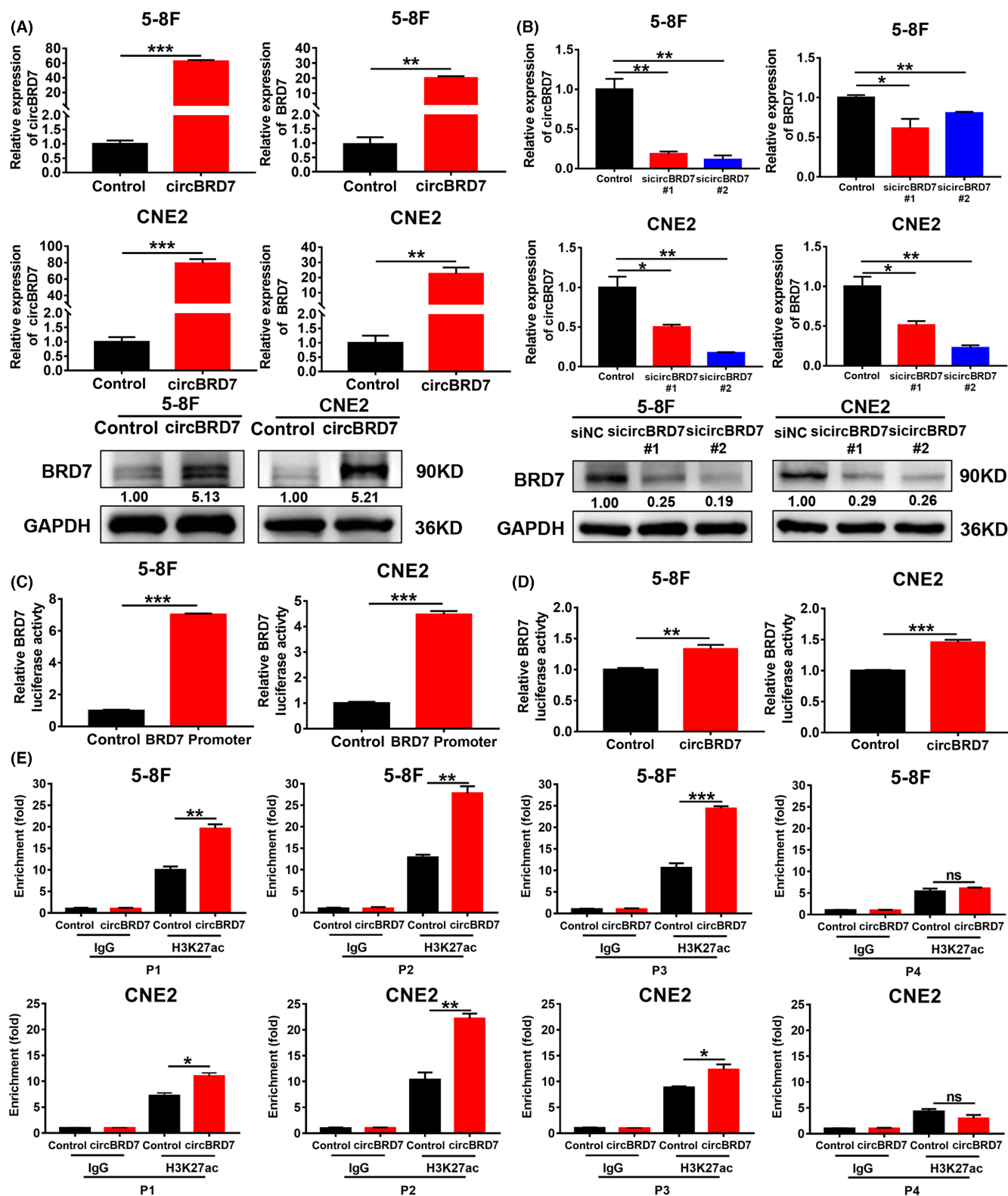


**FIGURE 4** CircBRD7 promotes the transcriptional activation of BRD7. (A) BRD7 expression was detected by RT-qPCR and western blot assays under circBRD7 overexpression. (B) RT-qPCR and western blot experiments were performed to detect the effect of silencing circBRD7 on BRD7 expression. (C, D) A dual luciferase reporter assay was performed to detect the luciferase activity of BRD7 promoter (C) and the effect of circBRD7 on BRD7 promoter activity (D). (E) ChIP-qPCR was used to determine the enrichment of H3K27ac in different regions of the BRD7 promoter and the effect of circBRD7 on the modification level of H3K27ac in BRD7 promoter fragments (–2000 to –1220bp). DNA isolated from immunoprecipitate was amplified by qPCR, and normal rabbit IgG was used as negative control. H3K27ac, histone 3 lysine 27 acetylation. Data are presented as mean  $\pm$  SEM. \* $p$  < 0.05; \*\* $p$  < 0.01; \*\*\* $p$  < 0.001; ns, no significance.



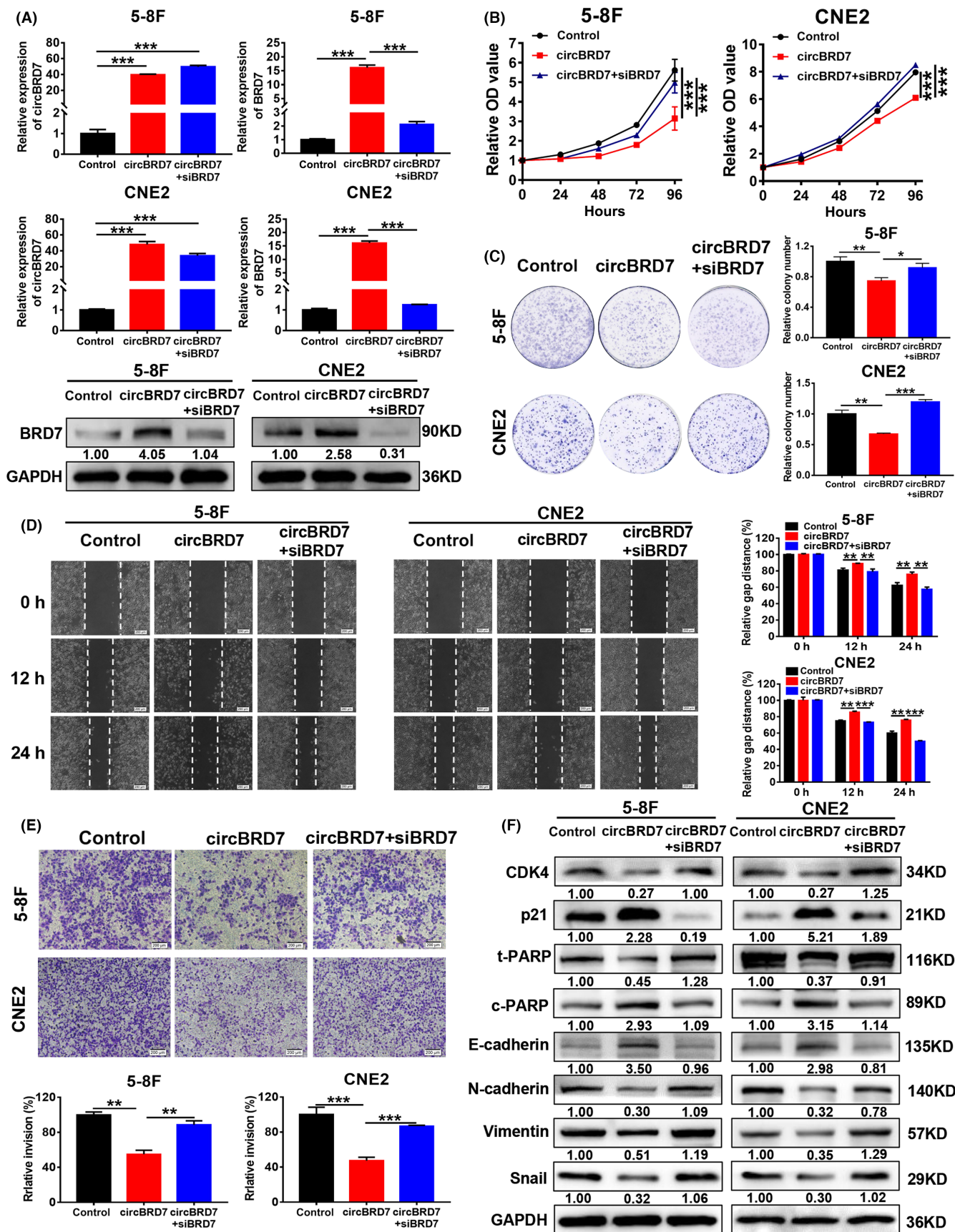


**FIGURE 5** Restoring BRD7 expression partially reverses the inhibitory effect of circBRD7 on the malignant phenotype of nasopharyngeal carcinoma (NPC) cells. (A) RT-qPCR and western blot were used to detect the expression of circBRD7 and BRD7 in each group. (B) The cell counting kit-8 (CCK-8) assay was used to detect the effects of circBRD7 overexpression and restoring BRD7 expression on the proliferation of NPC cells 5-8F and CNE2. (C–E) Representative and quantified results of the colony formation (C), wound healing (D), and transwell (E) assays in 5-8F and CNE2 cells. (F) Western blot was performed to detect the alterations of expression of cell cycle-, apoptosis- and epithelial–mesenchymal transition (EMT)-related molecules before and after BRD7 restoration. Data are presented as mean  $\pm$  SEM. \* $p < 0.05$ ; \*\* $p < 0.01$ ; \*\*\* $p < 0.001$ ; ns, no significance.

of BRD7 through the UCSC website and found that the promoter region of BRD7 was highly enriched with H3K27ac modification (Figure S6A), indicating that circBRD7 might upregulate BRD7 expression by enhancing H3K27ac modification in the BRD7 promoter region. Four pairs of primers (P1, P2, P3, and P4; Figure S6B) were further designed for the highly modified region of H3K27ac on the BRD7 promoter sequence. ChIP-qPCR results showed that H3K27ac was significantly enriched in the distal promoter region of BRD7 (–2000 to –1407) in 5-8F and CNE2 NPC cells. Moreover, circBRD7 overexpression enhanced H3K27ac modification of the BRD7 promoter region (Figure 4E), suggesting that circBRD7 promotes the transcriptional activation of BRD7 through enrichment of H3K27ac on its promoter region. Additionally, miR-498 and miR-944 were predicated to be the co-bound miRNAs with both circBRD7 and BRD7. Although overexpression of miR-498 and miR-944 decreased the expression of circBRD7, respectively, overexpression of miR-498 and miR-944 did not change the expression of BRD7 at the mRNA and protein levels. These results demonstrated that the miRNA sponge pathways mediated by miR-498 and miR-944 are not the mechanism of circBRD7 upregulating its host gene BRD7 (Figure S7). In addition, we further tested the effect of BRD7 on circBRD7 expression by RT-qPCR and found that BRD7 overexpression promoted the expression and formation of circBRD7 (Figure S6C), indicating that a positive feedback regulatory loop was formed between circBRD7 and BRD7, which might jointly participate in the inhibition of the malignant phenotype of NPC.

### 3.5 | Restoring BRD7 expression partially rescues the inhibitory effect of circBRD7 on the malignant phenotype of nasopharyngeal carcinoma cells

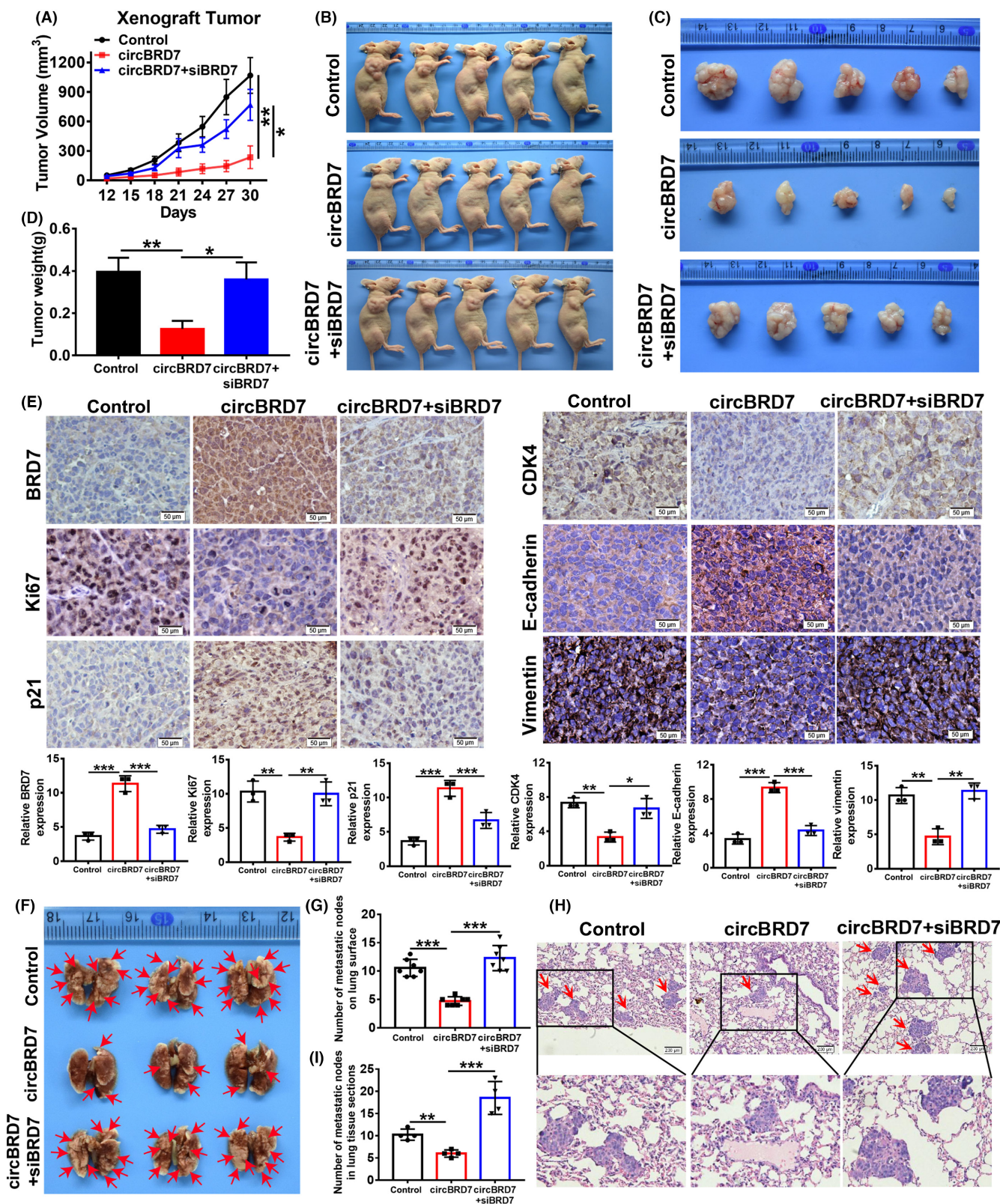
Given that circBRD7 inhibited the proliferation, migration, invasion, and EMT of NPC cells and positively regulated the expression

of its host gene at the transcriptional level, we sought to further investigate the effect of BRD7 on circBRD7-mediated malignant phenotype inhibition in NPC. SiBRD7 was transfected into circBRD7 overexpressed 5-8F and CNE2 cells to restore BRD7 expression, and quality control and confirmation were performed by RT-qPCR and western blot (Figure 5A). CCK-8 and colony formation assays showed that circBRD7 overexpression significantly inhibited the proliferation and colony formation of 5-8F and CNE2 cells, while restoration of BRD7 expression partially rescued the inhibitory effect of circBRD7 on cell proliferation and colony formation of NPC cells (Figure 5B,C). The results of flow cytometry analysis showed that circBRD7 overexpression inhibited cell cycle G1/S progression and promoted apoptosis. However, restoring BRD7 expression partially rescued the effect of circBRD7 on cell cycle arrest and apoptosis initiation (Figure 5B). Wound healing and transwell experiments confirmed that overexpression of circBRD7 sharply inhibited the migration and invasion of 5-8F and CNE2 cells, whereas restoring BRD7 expression partially restored the inhibitory effect of circBRD7 on the migration and invasion of NPC cells (Figure 5D,E).

We further detected the effect of restoring BRD7 expression on the expression of cell cycle-, apoptosis-, and EMT-related molecules in NPC. As a result, overexpression of circBRD7 inhibited the expression of CDK4, apoptosis marker t-PARP, and the mesenchymal markers N-cadherin, Vimentin, and Snail, while promoting the expression of cell cycle target molecule p21, apoptosis marker c-PARP, and the epithelial marker E-cadherin. Meanwhile, restoring BRD7 expression at least partially rescued the inhibitory effect of circBRD7 on CDK4, t-PARP, N-cadherin, Vimentin, and Snail, as well as the promotion effect on p21, c-PARP, and E-cadherin (Figure 5F and Figure S9). In conclusion, restoration of BRD7 expression at least partially rescues the inhibitory effect of circBRD7 on cell proliferation, migration, invasion, and EMT, which supports that circBRD7 inhibits the malignant phenotypes of NPC cells through positive regulation of its host gene expression.

**FIGURE 6** CircBRD7 attenuates tumor growth and metastasis in vivo by promoting its host gene expression. (A) Subcutaneous tumor growth curves in nude mice. (B) The images of nude mice in each group were photographed. (C) Images of subcutaneous tumor masses in each group after the nude mice were killed. (D) The tumor weights of each group ( $n = 5$  per group) were measured. (E) Representative images of immunohistochemical staining (IHC) staining for the expression of BRD7 and some cell proliferation, cell cycle, and epithelial–mesenchymal transition (EMT)-related molecules in xenograft tumor tissues (400 $\times$ , scale bar, 50  $\mu$ m). (F) Representative image of visible nodules on the lung surface of the metastatic tumor model in nude mice, with the red arrow representing pulmonary nodules. (G) The number of metastatic nodules on each lung surface was quantified, and each data point represents a nude mouse ( $n = 7$  per group). (H) Typical images of lung metastatic foci after H&E staining of lung tissue sections. Red arrows represent pulmonary nodules. (I) Quantitative statistical histogram of the number of pulmonary nodules in lung tissue sections of four nude mice. Data are presented as mean  $\pm$  SEM. \* $p < 0.05$ ; \*\* $p < 0.01$ ; \*\*\* $p < 0.001$ .





### 3.6 | CircBRD7 attenuates tumor growth and metastasis in vivo by promoting its host gene expression

To further determine the role of BRD7 in the circBRD7-mediated tumor suppressive role, we examined the influence of the circBRD7/

BRD7 regulatory axis on tumor growth and metastasis in vivo. We first generated a xenograft tumor model, and the results showed that overexpression of circBRD7 significantly inhibited the tumor growth rate and alleviated tumor weight compared with the control, while restoration of BRD7 expression rescued the inhibitory

effect of circBRD7 on subcutaneous tumor growth in nude mice (Figure 6A–D). Furthermore, the expression of proliferation-, cell cycle- and EMT-related molecules was detected in xenograft tumor tissues by IHC. As expected, overexpression of circBRD7 significantly increased the expression of BRD7, and the expression of BRD7 was also restored in the recovery group. Moreover, circBRD7 overexpression dramatically inhibited the expression of Ki67, CDK4, and Vimentin and promoted the expression of p21 and E-cadherin, while restoring BRD7 expression rescued the inhibitory or promoting effect of circBRD7 on the expression of the above molecules (Figure 6E). Altogether, the in vivo experimental results further demonstrated that circBRD7 inhibits tumor growth by positively regulating BRD7 expression.

We further generated a lung metastatic model. As a result, the number of pulmonary nodules in the lung tissues of nude mice in the circBRD7 overexpression group was significantly less than that in the control group, while restoring BRD7 expression reversed the inhibitory effect of circBRD7 on lung metastasis of NPC (Figure 6F,G). H&E staining results of lung tissue sections also confirmed that circBRD7 overexpression inhibited the number and size of lung metastasis foci in NPC, and the number and size of lung metastasis foci were significantly recovered in the group with restored BRD7 expression (Figure 6H,I). In conclusion, circBRD7 inhibits lung metastasis of NPC in vivo by positively regulating BRD7 expression.

### 3.7 | Expression and clinical correlation of circBRD7 and BRD7 in biopsy tissues of NPC at different stages

To better understand the clinical value of circBRD7 and BRD7 in NPC clinical samples, the expression of circBRD7 and BRD7 in 43 noncancerous NP patients and 78 clinical biopsy patients with different stages of NPC was detected by ISH and IHC, respectively. The results showed that both circBRD7 and BRD7 were expressed at low levels in NPC tissues, and the expression of circBRD7 and BRD7 in

clinical stages III and IV was significantly lower than that in stages I and II (Figure 7A,B). The expression levels of circBRD7 and BRD7 in these tissues were positively correlated ( $r=0.5014$ ;  $p<0.001$ ) (Figure 7C). The correlation between circBRD7 and BRD7 expression and their combined expression and the clinicopathological characteristics of NPC was further analyzed. As a result, circBRD7 and BRD7 had no significant correlation with the age and gender of NPC patients but had a significant negative correlation with clinical stage, and the combination of circBRD7 and BRD7 expression can better distinguish the clinical progression of NPC (Table 3). Furthermore, another set of independent fresh biopsies including eight noncancerous NP patients and 30 NPC patients was collected for the expression detection of circBRD7 and BRD7 by RT-qPCR. The results showed that the expression of circBRD7 and BRD7 in NPC patients was significantly lower than that in noncancerous NP tissues (Figure 7D,E). Pearson correlation analysis confirmed that circBRD7 and BRD7 expression were positively correlated ( $r=0.6776$ ;  $p<0.001$ ) (Figure 7F), which was consistent with the results detected in paraffin sections of NPC. Therefore, low circBRD7 expression and low BRD7 expression could be used as potential molecular markers for the evaluation of the malignant progression of NPC, and targeting circBRD7/BRD7 axis is expected to be a promising molecular strategy for the clinical diagnosis and treatment of NPC.

## 4 | DISCUSSION

Bromodomain-containing 7 was confirmed as a critical member of the bromodomain protein family and functions as a tumor suppressor in several tumors, such as NPC.<sup>6–10,19,29–32</sup> Increasing evidence has indicated that many protein-coding genes contain circular RNA forms, which play critical biological roles as oncogenes or tumor suppressors in the occurrence and development of NPC.<sup>13–17,33–35</sup> In this study, circBRD7 was identified as a circular RNA that is formed by reverse splicing of exons 6–8 of the BRD7 gene. Functional experiments confirmed that circBRD7 inhibited proliferation, colony

TABLE 3 Association between the expression of circBRD7, BRD7, and NPC clinical pathological features ( $n=78$ ).

Variables Features	circBRD7 expression			BRD7 expression			circBRD7/BRD7		
	Low	High	<i>p</i>	Low	High	<i>p</i>	L-L	H-H	<i>p</i>
Gender									
Male ( $n=52$ )	45 (87%)	7 (13%)	0.8181	43 (83%)	9 (17%)	0.4667	40 (77%)	4 (8%)	0.9571
Female ( $n=26$ )	22 (85%)	4 (15%)		23 (88%)	3 (12%)		21 (81%)	2 (8%)	
Age									
$\leq 47$ ( $n=41$ )	34 (83%)	7 (17%)	0.4275	35 (85%)	6 (15%)	0.8467	32 (78%)	4 (15%)	0.5054
$> 47$ ( $n=37$ )	33 (89%)	4 (11%)		31 (84%)	6 (16%)		29 (78%)	2 (5%)	
Clinical stages									
I–II ( $n=15$ )	10 (67%)	5 (33%)	0.0173*	9 (60%)	6 (40%)	0.0033**	7 (47%)	3 (20%)	0.0115*
III–IV ( $n=63$ )	57 (90%)	6 (10%)		57 (90%)	6 (10%)		54 (86%)	3 (5%)	

Note: Statistical analysis was performed using the  $\chi^2$ -test. \* $p<0.05$ ; \*\* $p<0.01$ .

Abbreviations: BRD7, bromodomain-containing protein 7; H, high expression; L, low expression; NPC, nasopharyngeal carcinoma.



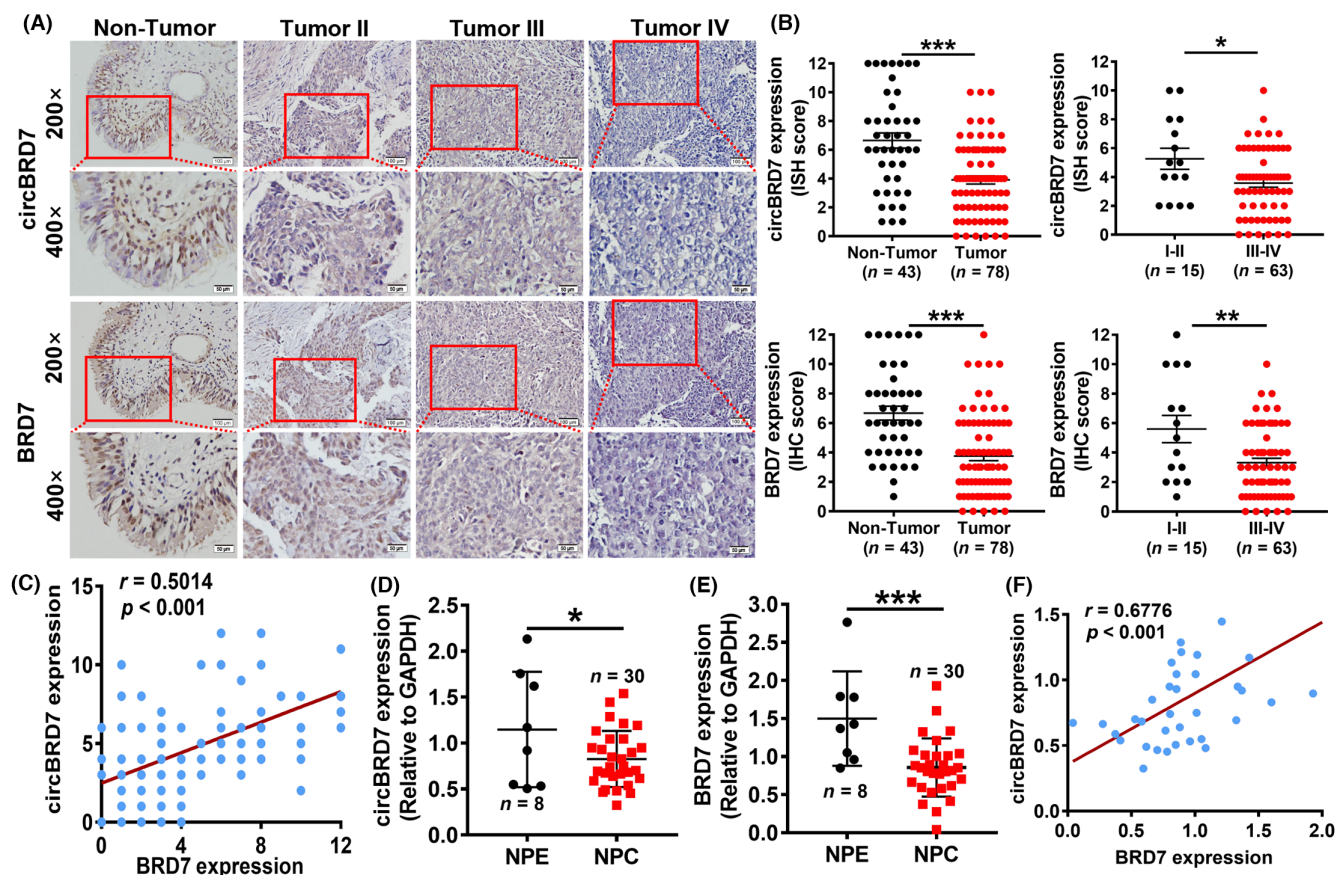


**FIGURE 7** Expression and clinical correlation of circBRD7 and BRD7 in biopsy tissues of nasopharyngeal carcinoma (NPC) at different stages. (A, B) Representative images (A) and statistical quantification charts (B) of in situ hybridization staining (ISH) and immunohistochemical staining (IHC) experiments to detect the expression of circBRD7 and BRD7 in noncancerous nasopharyngeal tissues and biopsies of NPC with different clinical TNM stages. (C) Correlation analysis between the expression of circBRD7 and its host gene BRD7 expression. (D) RT-qPCR was used to detect the expression of circBRD7 in eight noncancerous nasopharyngeal tissues and 30 biopsy tissues of NPC. (E) RT-qPCR was used to detect the expression of BRD7 in the same eight noncancerous nasopharyngeal tissues and 30 biopsy tissues of NPC. (F) Correlation analysis between the expression of circBRD7 and its host gene BRD7 expression in another set of independent fresh biopsies. Data are presented as mean  $\pm$  SEM. \* $p < 0.05$ ; \*\* $p < 0.01$ ; \*\*\* $p < 0.001$ .

formation, G1/S phase process, migration, and invasion of NPC cells, as well as tumor growth and metastasis in vivo, revealing that circBRD7 plays a role as a tumor suppressor in the occurrence and progression of NPC.

Increasing studies have reported that circRNAs can regulate the transcription, mRNA stability,<sup>36,37</sup> translation, and protein activity of host genes<sup>38-40</sup> and participate in tumor progression by positively or negatively regulating the expression of host genes.<sup>41</sup> In our study, circBRD7 was confirmed to be a circRNA encoded by BRD7 and promoted the expression of BRD7. CircBRD7 was mainly distributed in the nucleus, which suggested that circBRD7 may regulate its host gene at the transcriptional level. Many studies have demonstrated that ncRNAs can regulate gene expression by regulating the epigenetic characteristics of gene promoter regions.<sup>26,42</sup> Epigenetics and chromatin biology studies have demonstrated that active promoters have unique epigenetic markers, such as H3K27ac and H3K4me3, which can relax the chromatin state and then activate gene transcription.<sup>26-28</sup> As expected, H3K27ac modification

was found to be enriched in the BRD7 distal promoter region (~2000 to ~1407), while circBRD7 overexpression promoted the enrichment of H3K27ac in the BRD7 promoter region, thereby transcriptionally activating BRD7 expression. We speculated that circBRD7 may act as a scaffold to recruit histone acetyltransferase to the BRD7 promoter, thereby regulating the enrichment of H3K27ac histone markers in the BRD7 promoter region, but the detailed mechanism remains to be further studied. Furthermore, we investigated the effect of BRD7 on the circBRD7-mediated tumor suppressive role in NPC, and the results showed that restoring BRD7 expression at least partially reversed the inhibitory effect of circBRD7 on the malignant phenotypes of NPC. Therefore, we concluded that circBRD7 exerts a tumor suppressive function in NPC through positive regulation of BRD7 expression.

Unlike the forward splicing of linear pre-mRNA, circular RNA is formed by reverse splicing of pre-mRNA. Subsequently, we further discussed the influence of BRD7 overexpression on circBRD7 expression and found that overexpression of BRD7 accelerated the

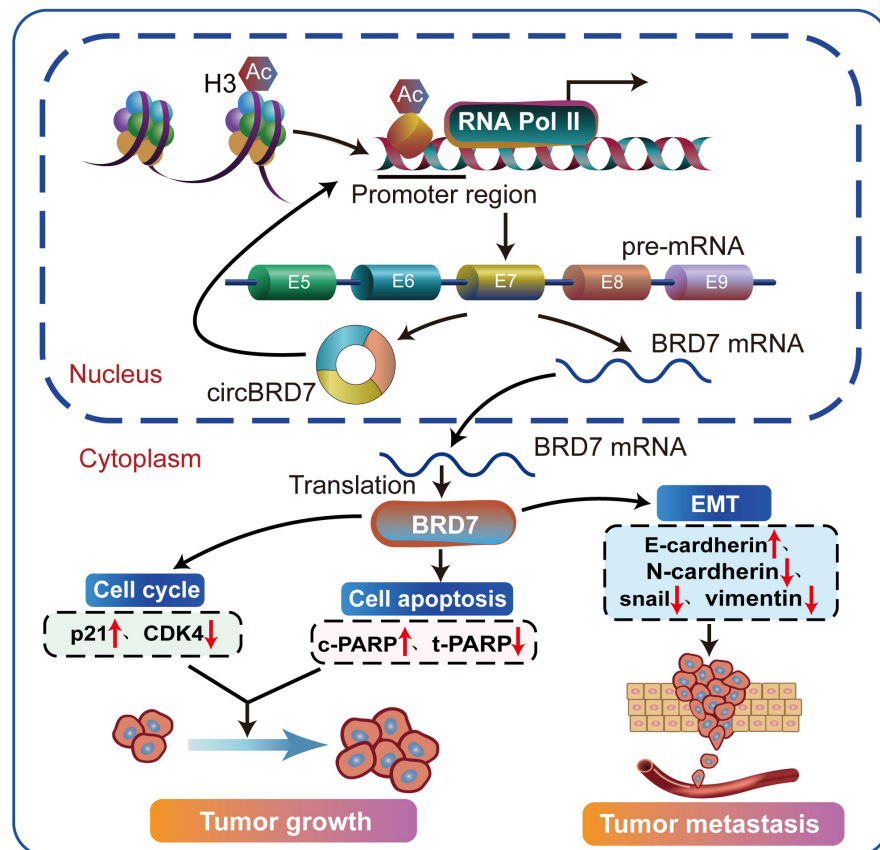


**FIGURE 8** Schematic diagram of the molecular mechanism of circBRD7 inhibiting the malignant progression of nasopharyngeal carcinoma (NPC). CircBRD7 is a circRNA formed by reverse splicing of exons 6–8 of the BRD7 and plays a tumor suppressive role in NPC by inhibiting the proliferation, migration, and invasion of NPC cells as well as xenograft tumor growth and metastasis. Mechanistically, circBRD7 enhanced the transcriptional activity of BRD7 by enhancing the enrichment of H3K27ac in its promoter region, and BRD7 promoted the expression of circBRD7. CircBRD7/BRD7 formed a positive feedback loop, thus inhibiting carcinogenesis and tumor progression in NPC. H3, histone 3; Ac, acetylation; EMT, epithelial-mesenchymal transition.

expression and formation of circBRD7 in NPC cells, suggesting that circBRD7 and BRD7 formed a positive feedback regulatory loop. As the formation and expression of circRNAs are comprehensively regulated by splicing factors, transcription factors, specific enzymes, cis-acting elements, and other factors,<sup>43–46</sup> we speculated that the positive feedback regulatory loop formed by circBRD7 and BRD7 might be involved in the carcinogenesis and tumor progression of NPC, where circBRD7 acts as a critical driving factor in the balance of the circBRD7/BRD7 regulatory axis (Figure 8). To further authenticate the expression and regulatory relationship as well as the clinical value of circBRD7 and BRD7, we collected noncancerous nasopharyngeal tissues and clinical biopsy tissues of NPC and confirmed that circBRD7 was expressed at low levels in NPC biopsy specimens, negatively correlated with TNM stage and positively correlated with BRD7 expression. Therefore, targeting the circBRD7/BRD7 axis is a promising strategy for the clinical diagnosis and treatment of NPC. For example, it is feasible for the researchers to develop a kind of nucleic acid drug or delivery system targeting circBRD7 to exert anti-tumor roles in tumors. In addition, a series of drugs targeting BRD7 could be developed to increase the expression or protein stability of BRD7, including the BRD7 expressing system, small molecule activators, and polypeptide drugs.

In conclusion, our study showed that circBRD7 is a circular RNA derived from BRD7 and functions as a tumor suppressor to inhibit cell proliferation, migration, invasion as well as the xenograft tumor growth and metastasis by enhancing the transcriptional activity and expression of BRD7. Targeting the circBRD7/

BRD7 axis is a potential strategy for the clinical diagnosis and treatment of NPC.

#### AUTHOR CONTRIBUTIONS

**Jianxia Wei:** Conceptualization; data curation; formal analysis; investigation; methodology; validation; visualization; writing – original draft; writing – review and editing. **Mengna Li:** Methodology; resources; writing – review and editing. **Shipeng Chen:** Resources; software. **Changning Xue:** Resources; writing – review and editing. **Lemei Zheng:** Resources; writing – review and editing. **Yumei Duan:** Resources; writing – review and editing. **Hongyu Deng:** Resources. **Songqing Fan:** Resources. **Wei Xiong:** Resources; supervision. **Ming Zhou:** Conceptualization; funding acquisition; methodology; project administration; supervision; writing – original draft; writing – review and editing.

#### ACKNOWLEDGMENTS

We thank Prof. Li Yong for providing pcDNA3.1(+) CircRNA Mini Vectors.

#### FUNDING INFORMATION

This study was supported by the grants from the National Natural Science Foundation of China (grant no. 82172592), the program of Introducing Talents of Discipline to Universities (grant no. 111–2–12).

#### CONFLICT OF INTEREST STATEMENT

The authors have no conflict of interest.

## ETHICS STATEMENTS

Approval of the research protocol by an Institutional Reviewer Board: This study was approved by Ethics Review Committees/Institutional Review Boards of Central South University (Changsha, China).

Informed Consent: All patients involved in this article signed informed consent.

Registry and the Registration No. of the study/trial: N/A.

Animal Studies: All the animal experiments in this study were approved by the Institutional Animal Care and Use Committee (IACUC) of Central South University.

## ORCID

Songqing Fan  <https://orcid.org/0000-0002-1486-9909>

Ming Zhou  <https://orcid.org/0000-0003-4938-5397>

## REFERENCES

- Chen YP, Chan ATC, Le QT, Blanchard P, Sun Y, Ma J. Nasopharyngeal carcinoma. *Lancet*. 2019;394(10192):64-80.
- Xu T, Tang J, Gu M, Liu L, Wei W, Yang H. Recurrent nasopharyngeal carcinoma: a clinical dilemma and challenge. *Curr Oncol*. 2013;20(5):e406-e419.
- Campion NJ, Ally M, Jank BJ, Ahmed J, Alusi G. The molecular march of primary and recurrent nasopharyngeal carcinoma. *Oncogene*. 2021;40(10):1757-1774.
- Yu Y, Xie Y, Cao L, et al. Isolation of tumor differentially expressed genes by mixing probes library screen. *Chin J Cancer*. 2001;2:4-82.
- Yu Y, Zhang BC, Xie Y, et al. Analysis and molecular cloning of differentially expressing genes in nasopharyngeal carcinoma. *Sheng Wu Hua Xue Yu Sheng Wu Wu Li Xue Bao (Shanghai)*. 2000;32(4):327-332.
- Zhou J, Ma J, Zhang BC, et al. BRD7, a novel bromodomain gene, inhibits G1-S progression by transcriptionally regulating some important molecules involved in ras/MEK/ERK and Rb/E2F pathways. *J Cell Physiol*. 2004;200(1):89-98.
- Peng C, Liu HY, Zhou M, et al. BRD7 suppresses the growth of nasopharyngeal carcinoma cells (HNE1) through negatively regulating beta-catenin and ERK pathways. *Mol Cell Biochem*. 2007;303(1-2):141-149.
- Zhou M, Xu XJ, Zhou HD, et al. BRD2 is one of BRD7-interacting proteins and its over-expression could initiate apoptosis. *Mol Cell Biochem*. 2006;292(1-2):205-212.
- Wu M, Li X, Li X, Li G. Signaling transduction network mediated by tumor suppressor/susceptibility genes in NPC. *Curr Genomics*. 2009;10(4):216-222.
- Wang H, Zhao R, Zhou M, et al. Preparation of polyclonal antibody highly specific for mouse BRD7 protein and its application. *Acta Biochim Biophys Sin (Shanghai)*. 2014;46(2):163-166.
- Memczak S, Jens M, Elefsinioti A, et al. Circular RNAs are a large class of animal RNAs with regulatory potency. *Nature*. 2013;495(7441):333-338.
- Lasda E, Parker R. Circular RNAs: diversity of form and function. *RNA*. 2014;20(12):1829-1842.
- Mo Y, Wang Y, Zhang S, et al. Circular RNA circRNF13 inhibits proliferation and metastasis of nasopharyngeal carcinoma via SUMO2. *Mol Cancer*. 2021;20(1):112.
- Tang L, Xiong W, Zhang L, et al. circSETD3 regulates MAPRE1 through miR-615-5p and miR-1538 sponges to promote migration and invasion in nasopharyngeal carcinoma. *Oncogene*. 2021;40(2):307-321.
- Hong X, Liu N, Liang Y, et al. Circular RNA CRIM1 functions as a ceRNA to promote nasopharyngeal carcinoma metastasis and docetaxel chemoresistance through upregulating FOXQ1. *Mol Cancer*. 2020;19(1):33.
- Li W, Lu H, Wang H, et al. Circular RNA TGFBR2 acts as a ceRNA to suppress nasopharyngeal carcinoma progression by sponging miR-107. *Cancer Lett*. 2021;499:301-313.
- Ge J, Wang J, Xiong F, et al. Epstein-Barr virus-encoded circular RNA CircBART2.2 promotes immune escape of nasopharyngeal carcinoma by regulating PD-L1. *Cancer Res*. 2021;81(19):5074-5088.
- Zhao R, Liu Y, Wu C, et al. BRD7 promotes cell proliferation and tumor growth through stabilization of c-Myc in colorectal cancer. *Front Cell Dev Biol*. 2021;9:659392.
- Li M, Wei Y, Liu Y, et al. BRD7 inhibits enhancer activity and expression of BIRC2 to suppress tumor growth and metastasis in nasopharyngeal carcinoma. *Cell Death Dis*. 2023;14(2):121.
- Liu Y, Zhao R, Wang H, et al. miR-141 is involved in BRD7-mediated cell proliferation and tumor formation through suppression of the PTEN/AKT pathway in nasopharyngeal carcinoma. *Cell Death Dis*. 2016;7(3):e2156.
- Zhan Y, Chen X, Zheng H, et al. YB1 associates with oncogenic roles and poor prognosis in nasopharyngeal carcinoma. *Sci Rep*. 2022;12(1):3699.
- Zhou J, Zhang S, Chen Z, He Z, Xu Y, Li Z. CircRNA-ENO1 promoted glycolysis and tumor progression in lung adenocarcinoma through upregulating its host gene ENO1. *Cell Death Dis*. 2019;10(12):885.
- Ye F, Gao G, Zou Y, et al. circFBXW7 inhibits malignant progression by sponging miR-197-3p and encoding a 185-aa protein in triple-negative breast cancer. *Mol Ther Nucleic Acids*. 2019;18:88-98.
- Feng Y, Yang Y, Zhao X, et al. Circular RNA circ0005276 promotes the proliferation and migration of prostate cancer cells by interacting with FUS to transcriptionally activate XIAP. *Cell Death Dis*. 2019;10(11):792.
- Chen N, Zhao G, Yan X, et al. A novel FLI1 exonic circular RNA promotes metastasis in breast cancer by coordinately regulating TET1 and DNMT1. *Genome Biol*. 2018;19(1):218.
- Zhang H, Zhang N, Liu Y, et al. Epigenetic regulation of NAMPT by NAMPT-AS drives metastatic progression in triple-negative breast cancer. *Cancer Res*. 2019;79(13):3347-3359.
- Rada-Iglesias A, Bajpai R, Swigut T, Brugmann SA, Flynn RA, Wysocka J. A unique chromatin signature uncovers early developmental enhancers in humans. *Nature*. 2011;470(7333):279-283.
- Kouzarides T. Chromatin modifications and their function. *Cell*. 2007;128(4):693-705.
- Park YA, Lee JW, Kim HS, et al. Tumor suppressive effects of bromodomain-containing protein 7 (BRD7) in epithelial ovarian carcinoma. *Clin Cancer Res*. 2014;20(3):565-575.
- Gao Y, Wang B, Gao S. BRD7 acts as a tumor suppressor gene in lung adenocarcinoma. *PLoS One*. 2016;11(8):e0156701.
- Zhu B, Tian J, Zhong R, et al. Genetic variants in the SWI/SNF complex and smoking collaborate to modify the risk of pancreatic cancer in a Chinese population. *Mol Carcinog*. 2015;54(9):761-768.
- Luo Y, Wang X, Niu W, et al. BRD7 stabilizes P53 via Dephosphorylation of MDM2 to inhibit tumor growth in breast cancer harboring wild-type P53. *J Cancer*. 2022;13(5):1436-1448.
- Wang Y, Yan Q, Mo Y, et al. Splicing factor derived circular RNA circCAMSAP1 accelerates nasopharyngeal carcinoma tumorigenesis via a SERPINH1/c-Myc positive feedback loop. *Mol Cancer*. 2022;21(1):62.
- Wei Z, Shi Y, Xue C, et al. Understanding the dual roles of CircHIPK3 in tumorigenesis and tumor progression. *J Cancer*. 2022;13(15):3674-3686.
- Xue C, Wei J, Li M, et al. The emerging roles and clinical potential of circSMARCA5 in cancer. *Cells*. 2022;11(19):3074.

36. Du WW, Yang W, Li X, et al. A circular RNA circ-DNMT1 enhances breast cancer progression by activating autophagy. *Oncogene*. 2018;37(44):5829-5842.
37. Zhao W, Wang S, Qin T, Wang W. Circular RNA (circ-0075804) promotes the proliferation of retinoblastoma via combining heterogeneous nuclear ribonucleoprotein K (HNRNPK) to improve the stability of E2F transcription factor 3 E2F3. *J Cell Biochem*. 2020;121(7):3516-3525.
38. Hu X, Wu D, He X, et al. circGSK3 $\beta$  promotes metastasis in esophageal squamous cell carcinoma by augmenting  $\beta$ -catenin signaling. *Mol Cancer*. 2019;18(1):160.
39. Wu N, Yuan Z, Du KY, et al. Translation of yes-associated protein (YAP) was antagonized by its circular RNA via suppressing the assembly of the translation initiation machinery. *Cell Death Differ*. 2019;26(12):2758-2773.
40. Du WW, Fang L, Yang W, et al. Induction of tumor apoptosis through a circular RNA enhancing Foxo3 activity. *Cell Death Differ*. 2017;24(2):357-370.
41. Wei J, Li M, Xue C, et al. Understanding the roles and regulation patterns of circRNA on its host gene in tumorigenesis and tumor progression. *J Exp Clin Cancer Res*. 2023;42(1):86.
42. Ma Y, Zheng W. H3K27ac-induced lncRNA PAXIP1-AS1 promotes cell proliferation, migration, EMT and apoptosis in ovarian cancer by targeting miR-6744-5p/PCBP2 axis. *J Ovarian Res*. 2021;14(1):76.
43. Conn SJ, Pillman KA, Toubia J, et al. The RNA binding protein quaking regulates formation of circRNAs. *Cell*. 2015;160(6):1125-1134.
44. Park OH, Ha H, Lee Y, et al. Endoribonucleolytic cleavage of m6A-containing RNAs by RNase P/MRP complex. *Mol Cell*. 2019;74(3):494-507.e8.
45. Ivanov A, Memczak S, Wyler E, et al. Analysis of intron sequences reveals hallmarks of circular RNA biogenesis in animals. *Cell Rep*. 2015;10(2):170-177.
46. Rybak-Wolf A, Stottmeister C, Glažar P, et al. Circular RNAs in the mammalian brain are highly abundant, conserved, and dynamically expressed. *Mol Cell*. 2015;58(5):870-885.

## SUPPORTING INFORMATION

Additional supporting information can be found online in the Supporting Information section at the end of this article.

**How to cite this article:** Wei J, Li M, Chen S, et al. CircBRD7 attenuates tumor growth and metastasis in nasopharyngeal carcinoma via epigenetic activation of its host gene. *Cancer Sci*. 2024;115:139-154. doi:[10.1111/cas.15998](https://doi.org/10.1111/cas.15998)